ELSEVIER

Inorganica Chimica Acta 228 (1995) 255–260

Inorganica Chimica Acta

Note

An X-ray diffraction study on the structure of solvated manganese(II) ion and manganese(II) complexes with pyridine, 3-methylpyridine and 4-methylpyridine in *N,N*-dimethylformamide

Makoto Kurihara, Kazuhiko Ozutsumi *, Takuji Kawashima

Laboratory of Analytical Chemistry, Department of Chemistry, University of Tsukuba, Tsukuba 305, Japan

Received 25 March 1994; revised 15 June 1994

Abstract

The structure of the solvated manganese(II) ion and the manganese(II) complexes with pyridine (py), 3-methylpyridine (3Me-py) and 4-methylpyridine (4Me-py) in *N,N*-dimethylformamide (DMF) has been studied by means of X-ray diffraction at 23 °C. It was revealed that the manganese(II) ion binds with six DMF molecules and has an octahedral structure in DMF. The Mn–O (DMF) bond length within $[Mn(dmf)_6]^{2+}$ is 221(1) pm, practically the same as that (220 pm) within $[Mn(H_2O)_6]^{2+}$ in water. The non-bonding Mn···C (DMF) distance is 315(2) pm and the Mn–O–C bond angle is thus 130°. It was also shown that the structure of $[Mn(L)]^{2+}$ (L = py, 3Me-py, 4Me-py) is octahedral in DMF. The Mn–O and Mn–N bond lengths are 222(1) pm for $[Mn(py)(dmf)_5]^{2+}$, 223(1) pm for $[Mn(3Me\text{-}py)(dmf)_5]^{2+}$ and 222(1) pm for $[Mn(4Me\text{-}py)(dmf)_5]^{2+}$, and are virtually the same as the Mn–O one within $[Mn(dmf)_6]^{2+}$. However, the non-bonding Mn···C (DMF) distances within $[Mn(L)(dmf)_5]^{2+}$ are longer (321–322 pm) and the corresponding Mn–O–C bond angles (134–135°) are wider than those within $[Mn(dmf)_6]^{2+}$. Thus, in DMF the steric interaction between DMF molecules and pyridines in the first coordination sphere of the manganese(II) ion is quite large.

Keywords: Crystal structures; Manganese complexes; Pyridine complexes; Pyridine-substituted complexes

1. Introduction

The manganese(II) and zinc(II) ions react with pyridine (py), 3-methylpyridine (3Me-py) and 4-methylpyridine (4Me-py) to form $[Mn(L)]^{2+}$, $[Zn(L)]^{2+}$ and $[Zn(L)_2]^{2+}$ (L = py, 3Me-py, 4Me-py) in *N,N*-dimethylformamide (DMF) [1]. The formation entropies of these complexes are largely negative [1] unlike corresponding 2,2′-bipyridine and urea complexes with divalent transition metal ions in DMF [2–5], where the entropy values are close to zero. These facts indicate the large steric interaction between DMF and pyridines around the manganese(II) and zinc(II) ions. It is thus interesting to obtain the conformational information on the solvent and ligand molecules in these complexes. In this report we describe the structure parameters of the manganese(II) complexes in DMF determined by the X-ray diffraction method. The thermodynamic parameters of the complexes are discussed in relation to their structures.

2. Experimental

2.1. Reagents

All chemicals used were of reagent grade. Manganese(II) perchlorate DMF solvate $[Mn(dmf)_6](ClO_4)_2$ was prepared and DMF, py, 3Me-py and 4Me-py were purified as described elsewhere [1]. **Caution**: be careful in handling $[Mn(dmf)_6](ClO_4)_2$ because of the possibility of explosion due to dryness and/or heating! Water content in DMF, py, 3Me-py and 4Me-py was checked by the Karl Fischer method to be under 120 ppm.

Four sample solutions were prepared for X-ray diffraction measurements. The composition of the sample solutions is summarized in Table 1. Solution A is a manganese(II) perchlorate DMF solution involving the solvated manganese(II) ion. Solutions B, C and D were

* Corresponding author.

SSDI 0020-1693(94)04174-T

Table 1
The composition (mol dm^{-3}), stoichiometric volume V per manganese atom and density ρ of the sample solutions

	A Mn^{2+}	B $[Mn(py)]^{2+}$	C $[Mn(3Me\text{-}py)]^{2+}$	D $[Mn(4Me\text{-}py)]^{2+}$
Mn^{2+}	1.052	1.034	1.037	1.037
L		2.045	2.025	2.321
ClO_4^-	2.104	2.068	2.074	2.073
DMF	12.09	10.03	9.592	9.280
V (10^9 pm^3)	1.579	1.606	1.601	1.602
ρ (g cm^{-3})	1.152	1.157	1.153	1.158

prepared by dissolving $[Mn(dmf)_6](ClO_4)_2$ along with py, 3Me-py and 4Me-py, respectively, in DMF. In the solutions $[Mn(L)]^{2+}$ (L=py, 3Me-py, 4Me-py) exists as a main species. All solutions were prepared and treated in a dry box under nitrogen atmosphere.

2.2. X-ray diffraction measurements

X-ray diffraction data were obtained on a RINT 1100S θ–θ type diffractometer (Rigaku) by using an Mo tube (λ=71.07 pm) at 23 °C. The accessible range of scattering angle 2θ was from 2 to 140°, which corresponded to the scattering vector s ($=4\pi\lambda^{-1}\sin\theta$) range of 0.3×10^{-2} to 16.6×10^{-2} pm^{-1}. Times required to accumulate 120 000 counts were recorded at each angle of 2θ and the measurement was repeated three times over the whole angle range. The method of data treatments was similar to that given in Ref. [6]. Calculations were performed by using the program KURVLR [7]. A least-squares refinement for determining the structure parameters, the distance r, the temperature factor b, and the frequency factor n, was carried out by comparing the observed and theoretical reduced intensities so as to minimize the error-square sum $\Sigma s^2\{i(s)_{obs}-i(s)_{calc}\}^2$ by using a non-linear least-squares program based on an algorithm proposed by Marquardt [8].

3. Results

The reduced intensities $i(s)$ multiplied by s and the radial distribution functions in the form $D(r)-4\pi r^2\rho_0$ for solutions A to D are shown in Figs. 1 and 2, respectively. In the $(D(r)-4\pi r^2\rho_0)$ curves, two large peaks are observed around 140 and 230 pm and two small humps around 320 and 440 pm. Other peaks probably due to intermolecular interactions were not analyzed in the present study. The first peak at 140 pm is ascribed to the C–H, C–N and C=O bonds within DMF and the Cl–O bonds within ClO_4^-. The C–H, C–C and C–N bonds within pyridines also contribute to the peak in the case of solutions B, C and D. The second peak at 230 pm is expected to be due to the

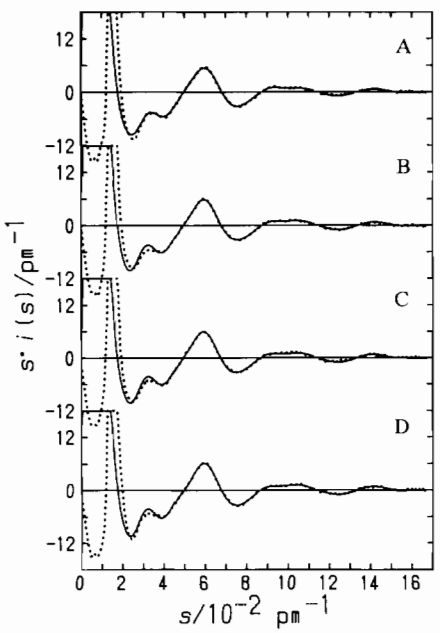

Fig. 1. The reduced intensities multiplied by s for sample solutions A to D. The observed $si(s)$ values are shown by dots and calculated ones by solid lines.

Mn–O and/or Mn–N bonds within the manganese(II) complexes. The non-bonding C···C, C···O and N···O interactions within DMF and the O···O contacts within ClO_4^- also contribute to the peak. The peak in the curve of solutions B, C and D further contains peaks due to the C···C and C···N interactions within pyridines. The third and fourth peaks at 320 and 440 pm may mainly be attributed to the non-bonding Mn···C (DMF) and Mn···N (DMF) interactions, respectively, the corresponding peaks having also been observed for the solvated copper(II) and cadmium(II) ions in DMF [9,10]. The Mn···N distance is well-defined because the rotation around the C–N bond is hindered by its double-bonding character. In order to extract peaks solely resulting from the intramolecular interactions within the manganese(II) complexes, the peak shapes due to the intramolecular interactions of DMF and ligand molecules and ClO_4^- should be subtracted from the observed radial distribution function. The structure

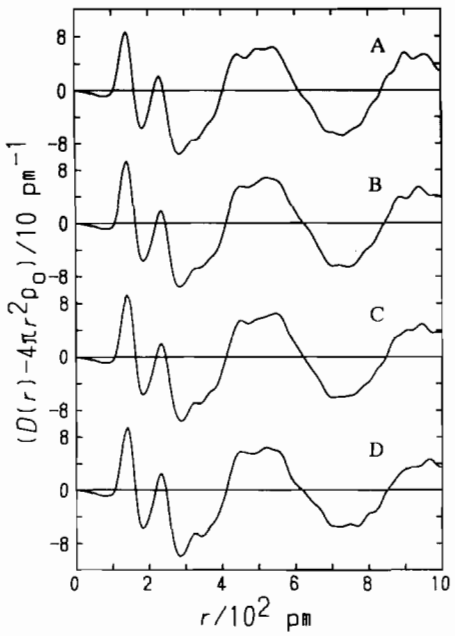

Fig. 2. The differential radial distribution functions, $D(r)-4\pi r^2\rho_0$, for sample solutions A to D.

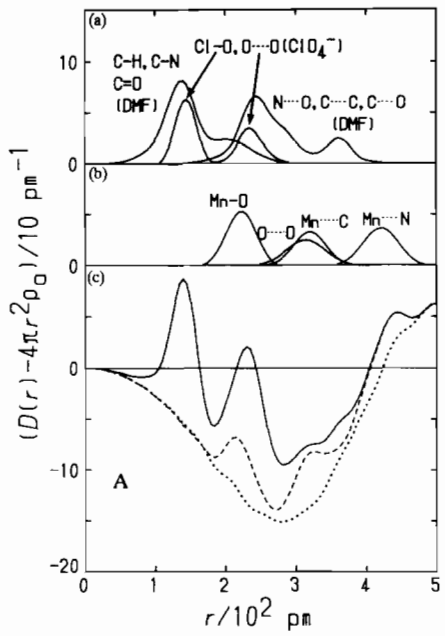

Fig. 3. The $(D(r)-4\pi r^2\rho_0)$ curve for the 1.052 mol dm^{-3} manganese(II) perchlorate DMF solution (solution A). (a) The theoretical peak shapes for intramolecular interactions within DMF molecules and perchlorate ions. (b) The peak shapes for the Mn–O, O···O, Mn···C and Mn···N interactions within the $[Mn(dmf)_6]^{2+}$ ion. (c) Dashed and dotted lines represent the residual curves after subtraction of the theoretical peaks in (a) and (a)+(b), respectively, from the original one (solid line).

Table 2
Structure parameters for py, 3Me-py and 4Me-py

	Interaction	r (pm)	b (10 pm^2)	n
py, 3Me-py, 4Me-py (pyridine ring)	C–N	133	1	2
	C–C	137	1	4
	C···N	237	3	2
	C···C	234	3	4
	C···C	269	5	2
	C···N	275	5	1
3Me-py	C–C	153	1	1
	C···C	241	2	2
	C···N	376	5	1
	C···C	373	5	1
	C···C	426	5	1
4Me-py	C–C	150	1	1
	C···C	241	3	2
	C···C	378	5	2
	C···N	430	5	1

parameters for DMF and ClO_4^- were quoted from the literature [11,12]. The intramolecular interatomic distances within py, 3Me-py and 4Me-py were evaluated from crystallographic data [13–20]. The distances are practically the same for several complexes of pyridines with different metal ions and thus the averaged values were used. The parameter values used are summarized in Table 2.

3.1. Structure of solvated manganese(II) ion

Fig. 3 shows the $(D(r)-4\pi r^2\rho_0)$ curve for solution A involving the solvated manganese(II) ion. Subtraction of the calculated peak shapes due to the intramolecular structure of DMF and ClO_4^- from the original curve (solid line) gives the residual curve (dashed line), in which three peaks remain at 220, 320 and 430 pm. The peaks solely originate from the intramolecular interactions within the solvated manganese(II) ion. The peak at 220 pm is ascribed to the Mn–O (DMF) bonds within the solvated manganese(II) ion, similar to the Mn–O (H_2O) bonds in water [21]. The peaks at 320 and 430 pm are due to the non-bonding Mn···C (DMF) and Mn···N (DMF) interactions within the solvated manganese(II) ion. The manganese(II) ion in DMF has been reported to have an octahedral structure according to EXAFS measurements [22]. In fact, the area under the peak at 220 pm corresponds to six Mn–O bonds. The octahedral structure of the manganese(II) ion is confirmed also by the X-ray diffraction method. Subtraction of the peaks due to the Mn–O, O···O, Mn···C and Mn···N interactions based on the octahedral $[Mn(dmf)_6]^{2+}$ structure leads to a smooth background curve (dotted line) with no distinct peak over the range $r<450$ pm.

In order to refine the structure parameters of $[Mn(dmf)_6]^{2+}$, a least-squares method was applied to the high-angle region of $si(s)$ values ($s>4\times10^{-2}$ pm^{-1}), where the intramolecular interactions within DMF, ClO_4^- and $[Mn(dmf)_6]^{2+}$ mainly contribute to the intensity values. In the course of the refinement, the structure parameters for DMF and ClO_4^- were fixed

at the literature values [11,12]. The interligand O···O distances were calculated from the optimized Mn–O distance based on the octahedral structure of the complex. In order to avoid errors introduced by neglecting long-range intermolecular interactions, the lower limit of the s value was varied from 4×10^{-2} to 6×10^{-2} pm^{-1}, but very similar results were obtained. The parameter values thus refined are given in Table 3 and the solid line calculated by using the parameter values reproduces well the experimental values over the range $s>4\times10^{-2}$ pm^{-1} as shown in Fig. 1.

3.2. Structure of manganese(II) pyridine complexes

Figs. 4, 5 and 6 show the $(D(r)-4\pi r^2\rho_0)$ curves for solutions B, C and D, respectively, and they were analyzed by a similar procedure to that employed for solution A. Subtraction of the calculated peak shapes due to the intramolecular interactions within DMF, pyridines and ClO_4^- leads to the residual curve (dashed line in Figs. 4(d), 5(d) and 6(d)), where a peak remains at 220 pm. Although solutions B, C and D contain comparable amounts of $[Mn(dmf)_6]^{2+}$ and $[Mn(L)]^{2+}$, the area under the peak corresponds to six Mn–O or Mn–N bonds, regardless of different assumptions of the concentration ratio of $[Mn(dmf)_6]^{2+}$ to $[Mn(L)]^{2+}$. The $[Mn(L)]^{2+}$ complexes in DMF are thus concluded to have a six-coordinated octahedral structure. The amount of $[Mn(dmf)_6]^{2+}$ was evaluated to be 50, 40 and 30 mol% in solutions B, C and D, respectively, on the basis of stability constants [1]. Subtraction of the calculated peak shapes due to $[Mn(dmf)_6]^{2+}$ leads to the residual curve (chain line in Figs. 4(d), 5(d) and 6(d)). Since it is difficult to distinguish one Mn–N (pyridines) bond from five Mn–O (DMF) ones by the X-ray diffraction method, the peak remaining at 220 pm was analyzed by the assumption that the peak consists solely of the Mn–O bonds. The peak was well reproduced by assuming six Mn–O bonds with the length of 220 pm. Further subtraction of the peaks due to the O···O, Mn···C and Mn···N interactions based on the octahedral $[Mn(L)(dmf)_5]^{2+}$ structure leads to smooth background curve (dotted line in Figs. 4(d), 5(d) and 6(d)).

The structure parameters of the manganese(II) complexes were finally determined by a least-squares calculation. Since it is difficult to distinguish one py molecule from five DMF molecules within $[Mn(L)(dmf)_5]^{2+}$, the Mn–N (pyridines) bond was regarded as one of the six Mn–O (DMF) bonds. The assumption of the same distance for the Mn–O and Mn–N bonds is not unreasonable because the M–O and M–N bond distances are similar in lower complexes partially coordinated with ligands [23–25], though the distances differ significantly in the highest complexes fully coordinated [21,23–27]. Also, the Mn···C (DMF) and Mn···N (DMF) interactions included two Mn···C (pyridines, Mn–N–C) and two Mn···C (pyridines, Mn–N–C–C) interactions, respectively. Thus, in the course of the least-squares calculations, the structure parameters of six Mn–O, seven Mn···C and seven Mn···N interactions were optimized. No significant error could be introduced by this treatment since the X-ray scattering power of carbon, nitrogen and oxygen atoms are similar. Other assumptions adopted are the same as those for solution A. The parameters values determined are given in Table 3.

Table 3
Structure parameters for the manganese(II) complexes in *N,N*-dimethylformamide [a]

Interaction	Parameter	A Mn^{2+}	B $[Mn(py)]^{2+}$	C $[Mn(3Me\text{-}py)]^{2+}$	D $[Mn(4Me\text{-}py)]^{2+}$
Mn–O	r (pm)	221(1)	222(1)	223(1)	222(1)
	b (10 pm^2)	10(1)	24(2)	18(2)	17(2)
	n	6 [b]	6 [b]	6 [b]	6 [b]
O···O	r [c] (pm)	313	314	316	314
	b (10 pm^2)	20 [b]	20 [b]	20 [b]	20 [b]
	n	12 [b]	12 [b]	12 [b]	12 [b]
Mn···C	r (pm)	315(2)	322(2)	322(2)	321(1)
	b (10 pm^2)	25(3)	16(3)	12(3)	8(1)
	n	6 [b]	7 [b]	7 [b]	7 [b]
Mn···N	r (pm)	425(2)	435(3)	435(3)	437(2)
	b (10 pm^2)	16(2)	24(5)	23(5)	22(4)
	n	6 [b]	7 [b]	7 [b]	7 [b]
∠Mn–O–C	(°)	130	135	134	134

[a] Standard deviations are given in parentheses.
[b] The values were kept constant during the calculation.
[c] $r(O\cdots O)=\sqrt{2}r(Mn\text{–}O)$.

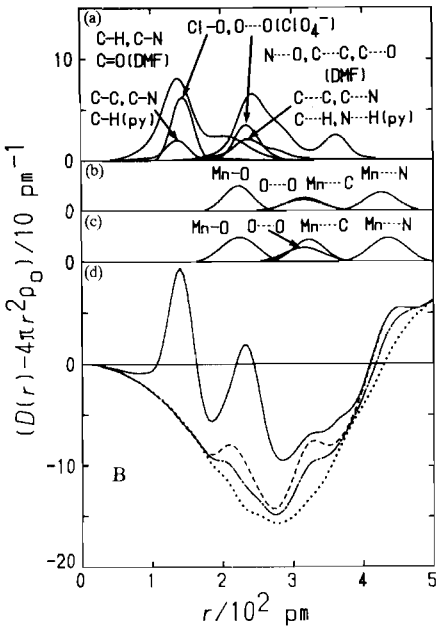

Fig. 4. The $(D(r)-4\pi r^2\rho_0)$ curve for the 1.034 mol dm^{-3} manganese(II) perchlorate DMF solution containing 2.045 mol dm^{-3} py (solution B). (a) The theoretical peak shapes for intramolecular interactions within DMF and py molecules and perchlorate ions. (b) The peak shapes for the Mn–O, O···O, Mn···C and Mn···N interactions within the $[Mn(dmf)_6]^{2+}$ ion. (c) The peak shapes for the Mn–O, O···O, Mn···C and Mn···N interactions within the $[Mn(py)(dmf)_5]^{2+}$ complex. (d) Dashed, chain and dotted lines represent the residual curves after subtraction of the theoretical peaks in (a), (a)+(b) and (a)+(b)+(c), respectively, from the original one (solid line).

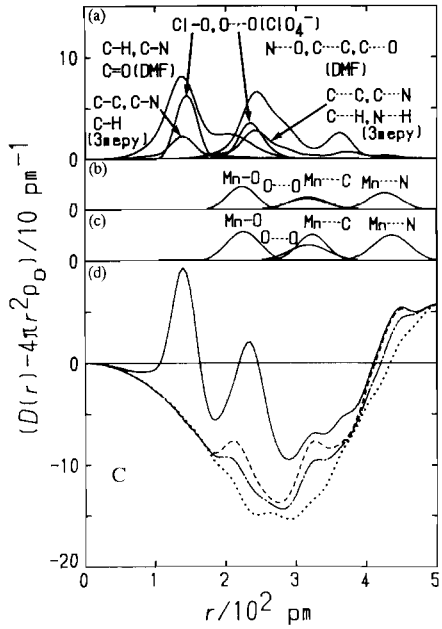

Fig. 5. The $(D(r)-4\pi r^2\rho_0)$ curve for the 1.037 mol dm^{-3} manganese(II) perchlorate DMF solution containing 2.025 mol dm^{-3} 3Me-py (solution C). (a) The theoretical peak shapes for intramolecular interaction within DMF and 3Me-py molecules and perchlorate ions. (b) The peak shapes for the Mn–O, O···O, Mn···C and Mn···N interactions within the $[Mn(dmf)_6]^{2+}$ ion. (c) The peak shapes for the Mn–O, O···O, Mn···C and Mn···N interactions within the $[Mn(3Me\text{-}py)(dmf)_5]^{2+}$ complex. (d) Dashed, chain and dotted lines represent the residual curves after subtraction of the theoretical peaks in (a), (a)+(b) and (a)+(b)+(c), respectively, from the original one (solid line).

4. Discussion

The Mn–O and/or Mn–N bond distances within $[Mn(dmf)_6]^{2+}$ and $[Mn(L)(dmf)_5]^{2+}$ (L=py, 3Me-py and 4Me-py) are the same within experimental uncertainties. However, the Mn···C and Mn···N distances within $[Mn(L)(dmf)_5]^{2+}$ are longer than those within $[Mn(dmf)_6]^{2+}$. The difference in the Mn···C and Mn···N distances between $[Mn(L)(dmf)_5]^{2+}$ and $[Mn(dmf)_6]^{2+}$ is ascribed to the different Mn–DMF interactions in the former complex from those in the latter. The Mn–O–C bond angles are estimated to be 130° for $[Mn(dmf)_6]^{2+}$ and 134–135° for $[Mn(L)(dmf)_5]^{2+}$. On the other hand, the Cu···C (DMF) and Cu···N (DMF) distances within $[Cu(dmf)_6]^{2+}$, $[CuCl(dmf)_5]^{+}$ and $[Cu(NO)_3(dmf)_5]^{+}$ are practically unchanged in DMF [9,28]. This fact indicates the large steric interaction between the DMF and ligand molecules in $[Mn(L)(dmf)_5]^{2+}$. Hence, the restriction of the DMF molecules around the manganese(II) ion is expected to be larger in $[Mn(L)(dmf)_5]^{2+}$ than $[Mn(dmf)_6]^{2+}$.

The entropies for the formation of $[Mn(L)(dmf)_5]^{2+}$ (L=py, 3Me-py, 4Me-py) in DMF are −57, −50 and −66 J K^{-1} mol^{-1} [1]. The DMF molecules solvating to the manganese(II) ion lose their freedom of motion to a considerable extent and the DMF molecules released from the solvation sphere upon complexation enter a structureless bulk solvent to lead to a large entropy gain. In fact, the halogeno complexation of the manganese(II) ion in DMF is accompanied by a large and positive entropy change [29,30]. Desolvation of anions also contributes to the positive entropy value. However, the entropy changes are appreciably negative for the formation of $[Mn(L)(dmf)_5]^{2+}$. Solvation of non-charged molecules such as pyridines is weaker than that of anions and the ligand molecules appreciably lose their freedom of motion upon complexation. Thus, the entropy changes are expected to have a value close to zero as found in the case of 2,2′-bipyridine and urea complexes with divalent transition metal ions [2–5]. Moreover, since py, 3Me-py and 4Me-py molecules are bulky, the motion of the DMF molecules is more restricted in $[Mn(L)(dmf)_5]^{2+}$ than $[Mn(dmf)_6]^{2+}$, which is directly confirmed by the structural analysis in the present study. Thus, the negative entropy changes result.

The stability of $[Mn(L)(dmf)_5]^{2+}$ (L=py, 3Me-py, 4Me-py) in DMF increases with increasing basicity of the nitrogen atom, showing a good linear free energy

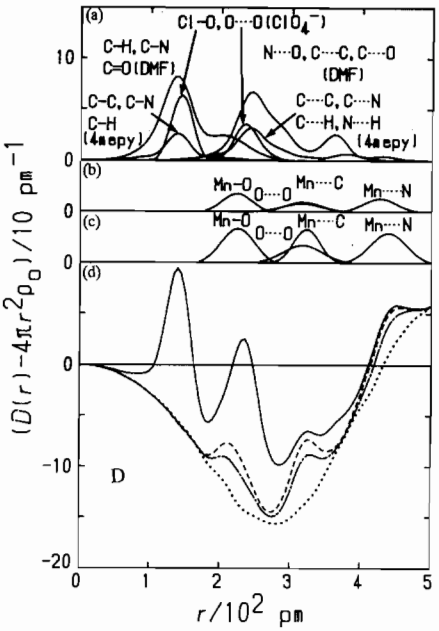

Fig. 6. The $(D(r)-4\pi r^2\rho_0)$ curve for the 1.037 mol dm^{-3} manganese(II) perchlorate DMF solution containing 2.321 mol dm^{-3} 4Me-py (solution D). (a) The theoretical peak shapes for intramolecular interactions within DMF and 4Me-py molecules and perchlorate ions. (b) The peak shapes for the Mn–O, O···O, Mn···C and Mn···N interactions within the $[Mn(dmf)_6]^{2+}$ ion. (c) The peak shapes for the Mn–O, O···O, Mn···C and Mn···N interactions within the $[Mn(4Me\text{-}py)(dmf)_5]^{2+}$ complex. (d) Dashed, chain and dotted lines represent the residual curves after subtraction of the theoretical peaks in (a), (a) + (b) and (a) + (b) + (c), respectively, from the original one (solid line).

relationship, but the enthalpy and entropy values for the formation of $[Mn(3Me\text{-}py)(dmf)_5]^{2+}$ deviate [1]. The formation of the 3Me-py complex is enthalpically less favorable but is entropically more favorable than the py and 4Me-py complexes. This suggests the weaker interaction of 3Me-py with the manganese(II) ion than that of py and 4Me-py though the deviation is rather small. Because the Mn–O and/or Mn–N bond lengths are the same for all complexes, the weaker interaction of 3Me-py is probably caused by a steric interaction between the 3Me-py and DMF molecules at a position apart from the manganese(II) ion in $[Mn(3Me\text{-}py)(dmf)_5]^{2+}$.

References

[1] M. Kurihara, K. Ozutsumi and T. Kawashima, *J. Chem. Soc., Dalton Trans.*, (1993) 3379.
[2] S. Ishiguro, L. Nagy and H. Ohtaki, *Bull. Chem. Soc. Jpn., 60* (1987) 2053.
[3] S. Ishiguro, L. Nagy and H. Ohtaki, *Bull. Chem. Soc. Jpn., 60* (1987) 2865.
[4] S. Ishiguro, K. Ozutsumi, L. Nagy and H. Ohtaki, *J. Chem. Soc., Dalton Trans.*, (1989) 655.
[5] K. Ozutsumi, Y. Taguchi and T. Kawashima, submitted for publication.
[6] J. Ohtaki, *Rev. Inorg. Chem., 4* (1982) 103.
[7] G. Johansson and M. Sandström, *Chem. Scr., 4* (1973) 195.
[8] D.M. Marquardt, *J. Soc. Ind. Appl.. Math., 11* (1963) 431.
[9] K. Ozutsumi, S. Ishiguro and H. Ohtaki, *Bull. Chem. Soc. Jpn., 61* (1988) 945.
[10] K. Ozutsumi, T. Takamuku, S. Ishiguro and H. Ohtaki, *Bull. Chem. Soc. Jpn., 62* (1989) 1875.
[11] H. Ohtaki, S. Itoh, T. Yamaguchi, S. Ishiguro and B.M. Rode, *Bull. Chem. Soc. Jpn., 56* (1983) 3406.
[12] H. Ohtaki and M. Maeda, *Bull. Chem. Soc. Jpn., 47* (1974) 2197.
[13] P.J. Clarke and H.J. Milledge, *Acta Crystallogr., Sect. B, 31* (1975) 1543.
[14] M.A. Hitchman and R. Thomas, *J. Chem. Soc., Dalton Trans.*, (1983) 2273.
[15] E.W. Ainscough, A.G. Bingham and A.M. Brodie, *J. Chem. Soc., Dalton Trans.*, (1984) 898.
[16] M. Taniguchi, Y. Sugita and A. Ouchi, *Bull. Chem. Soc. Jpn., 60* (1987) 1321.
[17] P. Roman, M.E. González-Aguado, C. Esteban-Calderón and M. Martínez-Ripoll, *Inorg. Chim. Acta, 90* (1984) 115.
[18] M. Laing and G. Carr, *Acta Crystallogr., Sect. B, 31* (1975) 2683.
[19] M. Taniguchi, M. Shimoi and A. Ouchi, *Bull. Chem. Soc. Jpn., 59* (1986) 2299.
[20] H. Lynton and M.C. Sears, *Can. J. Chem., 49* (1971) 3481.
[21] H. Ohtaki, T. Yamaguchi and M. Maeda, *Bull. Chem. Soc. Jpn., 49* (1976) 701.
[22] K. Ozutsumi, M. Koide, H. Suzuki and S. Ishiguro, *J. Phys. Chem., 97* (1993) 500.
[23] T. Fujita and H. Ohtaki, *Bull. Chem. Soc. Jpn., 55* (1982) 455.
[24] K. Ozutsumi and H. Ohtaki, *Bull. Chem. Soc. Jpn., 56* (1983) 3635.
[25] K. Ozutsumi and H. Ohtaki, *Bull. Chem. Soc. Jpn., 58* (1985) 1651.
[26] R.J. Doedens and L.F. Dahl, *J. Am. Chem. Soc., 88* (1966) 4847.
[27] T. Fujita and H. Ohtaki, *Bull. Chem. Soc. Jpn., 52* (1979) 3539.
[28] K. Ozutsumi, S. Ishiguro and H. Ohtaki, *Bull. Chem. Soc. Jpn., 61* (1988) 715.
[29] S. Ishiguro, K. Ozutsumi and H. Ohtaki, *J. Chem. Soc., Faraday Trans. 1, 84* (1988) 2409.
[30] K. Ozutsumi and S. Ishiguro, *J. Chem. Soc., Faraday Trans., 86* (1990) 271.